INFN - Laboratori Nazionali di Frascati, May 1995
From: **The Second DaΦne Physics Handbook**[1]
Chapter 5: The $\pi\pi$ Interaction
Eds. L. Maiani, G. Pancheri, N. Paver

# Low Energy $\pi\pi$ Scattering

**D. Morgan**

Particle Physics Department, Rutherford Appleton Laboratory,

Chilton, Didcot, Oxon OX11 0QX, U.K.

and

**M.R. Pennington**

Centre for Particle Theory, University of Durham, Durham DH1 3LE, U.K.

## 1 Introduction

The pion is the lightest hadron. Its mass is small on the scale of hadron physics, typically the proton mass. Though pions are obviously strongly interacting, low energy $\pi\pi$ scattering is weak. This has long been attributed to the pion being a (pseudo-) Goldstone boson associated with the spontaneous breakdown of chiral symmetry [1]. Not only does this explain the near masslessness of the pion, but imposes the vanishing at threshold of $\pi\pi$ scattering, with one pion off-shell [2]. Though this Adler zero does appear on-shell in physical $\pi\pi$ scattering, and so this consequence of chiral dynamics is a feature of the real world, its position depends on the details of the explicit breaking of chiral symmetry. This is embodied differently in different models [3, 4]. The fact that experiment still cannot decide between these has made this a live issue in the 1990's, despite the many sources of $\pi\pi$ final states.

[1]Supported by the INFN, by the EC under the HCM contract number CHRX-CT920026 and by the authors home institutions

The task of extracting $\pi\pi$ information from experiment is handicapped by the absence of direct $\pi\pi$ scattering measurements, but favoured by various simplifying features of the partial wave structure. This means there is unusual scope for exploiting S-matrix principles [5] in $\pi\pi$ phenomenology. Such methods help to compensate for the gaps and uncertainties introduced by the rather complicated recipes needed to pass from what is actually measured to inferred $\pi\pi$ scattering 'information'.

The layout of this short review is as follows : S-matrix methods are described in Sect. 2 and how one derives cross-sections for $\pi\pi$ scattering from experiment in Sect. 3. Conclusions on low energy $\pi\pi$ scattering from existing measurements are summarized in Sect. 4. Future experiments at DA$\Phi$NE should yield important new information on several relevant processes, notably $K_{e4}$ decays and $\gamma\gamma \to \pi\pi$. These are mentioned briefly in Sect. 4 and in greater detail elsewhere in this Handbook.

Like all low energy hadron processes, $\pi\pi$ scattering is dominated by resonances : the $I = 1$ channel has the $\rho-$resonance — a prime example of a quark model state. However the composition of the $I = 0$ resonances, the broad $f_0(\epsilon(1300))$ and narrower $f_0(S^*(980))$ [6], is still controversial. Since our focus is the near threshold region of $\pi\pi$ scattering accessible at DA$\Phi$NE, we do not consider these here.

# 2 S-matrix methods

(a) Correlating and interpolating $\pi\pi$ scattering data

The S-matrix constraints of analyticity, crossing and unitarity are exceptionally useful for $\pi\pi$ phenomenology [5, 7, 8]. It is the simplicity of $\pi\pi$ scattering that makes these constraints so powerful and easy to apply. This can be exploited to compensate for the indirect way that $\pi\pi$ scattering information is obtained.

We start here with a brief account of S-matrix methods. As usual one defines the Mandelstam variables $s, t$ and $u$ for the process $12 \to 34$ and its crossing variants $1\overline{3} \to 2\overline{4}$ and $1\overline{4} \to 2\overline{3}$ (Fig. 1). These obey the familiar relation $s + t + u = 4m_\pi^2$. For the $s$-channel reaction, $s \equiv (p_1 + p_2)^2$ is the CM energy squared, whilst $t$ and $u$ are the squared momentum transfers respectively from '1' to '3' and from '1' to '4'. With $\theta$ the $s-$channel CM scattering angle and $q$ the 3-momenta of the pions, then $t(u) = -2q^2(1 \mp \cos\theta)$.

Before getting into detail, it is worth recalling the general thrust of S-matrix principles

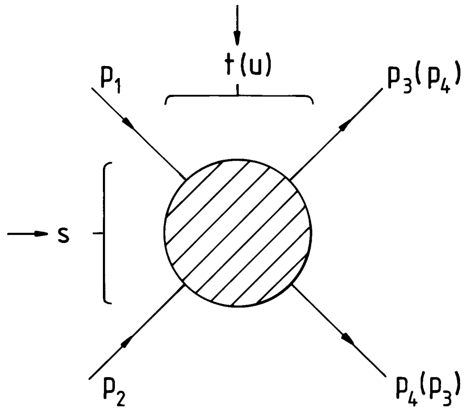


Figure 1: $s, t$ and $u$ variables for $\pi\pi$ scattering.

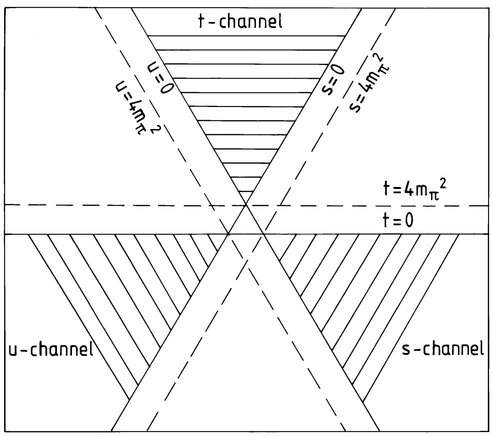


Figure 2: $s - t - u$ plane for $\pi\pi$ scattering; the shaded wedges indicate the physical regions.

and how they combine to restrict possibilities. Crossing properties are of obvious importance for $\pi\pi$ scattering because this process transforms into itself under crossing (Fig. 1), albeit with a mixing of isospin ($\pi^+\pi^+$ scattering becomes $\pi^+\pi^-$ scattering for example). Furthermore, because of the lightness of the pion, the $s, t$ and $u$ channel physical regions are close to each other on the typical hadronic energy scale of $O(1\text{ GeV})$ (Fig. 2). This underpins the well-known correlations between low energy parameters to be discussed below. With $T^{xI}$ denoting the $\pi\pi$ amplitude of isospin $I$ in the channel $x$, the general formula that expresses $s-u$ crossing, for example, is

$$T^{sI}(s,t,u) = \sum_{I'} C^{su}_{II'}\, T^{uI'}(u,t,s) \leftrightarrow (I, I' = 0, 1, 2) \tag{1}$$

where

$$C^{su}_{II'} = \begin{bmatrix} 1/3 & -1 & 5/3 \\ -1/3 & 1/2 & 5/6 \\ 1/3 & 1/2 & 1/6 \end{bmatrix}_{II'} \quad . \tag{2}$$

To extrapolate the $T^{sI}$ from one physical region to another one has to take account of their analyticity properties, in particular, the cut structure implied by unitarity. It is the interplay of analyticity with unitarity that allows the low energy amplitudes to be determined. Unitarity singles out the partial wave amplitudes, $t^I_J(s)$, defined by the Legendre expansion

$$T^I_s(s,t,u) \;=\; 32\pi \sum_{(J+I)even} (2J+1)\; t^I_J(s) P_J(\cos\theta) \tag{3}$$

where $\cos\theta \equiv (t-u)/4m^2_\pi$ . Our notation accords with work on Chiral Perturbation Theory [3] and not that generally used for $\pi\pi$ scattering [7]. In the standard normalization, the requirement of unitarity in the elastic region (for energies below $4\pi$ threshold), is

$$\mathrm{Im}\, t^I_J = \rho \mid t^I_J \mid^2 , \tag{4}$$

with

$$\rho = \sqrt{1 - 4m^2_\pi/s} \quad . \tag{5}$$

This relation is satisfied by the familiar parameterization in terms of the corresponding phase shifts, $\delta^I_J$,

$$t^I_J(s) = \exp(i\delta^I_J(s)) \sin\delta^I_J(s)/\rho \quad . \tag{6}$$

Above inelastic threshold, additional contributions appear on the right hand side of Eq. (4).

Near threshold, it is often convenient to write the partial wave amplitudes as functions of $q$, the CM 3-momentum, where $q^2 = s/4 - m_\pi^2$. Thus, scattering lengths and slope parameters are defined for each partial wave by the formula

$$\text{Re } t_J^I = q^{2J} \left(a_J^I + b_J^I q^2 + O(q^4)\right) . \tag{7}$$

The $S$ and $P$-wave scattering lengths are of special importance since they feature in predictions from chiral symmetry and current algebra. These are discussed by Gasser in the context of standard Chiral Perturbation Theory [9]. Generic features of such predictions are brought out in the lowest order version, or equivalently in Weinberg's simple current algebra scheme [10]. According to this model, the full amplitudes near threshold are of the form

$$\begin{aligned} T^0 &= 2c\left(s - m_\pi^2/2\right) \\ T^1 &= c\,(t-u) \\ T^2 &= c\left(2m_\pi^2 - s\right) \end{aligned} \tag{8}$$

with $c = 1/F_\pi^2 \approx 2.20 m_\pi^{-2}$. The pion decay constant $F_\pi$ is taken to have the value 92.4 MeV [9]. This yields scattering lengths in pion mass units :

$$a_0^0 = 0.159, \quad a_0^2 = -0.045, \quad a_1^1 = 0.030 \,, \tag{9}$$

and predicts zeros for $T^0$ and $T^2$ just below threshold, respectively at $m_\pi^2/2$ and $2m_\pi^2$. These are interpreted as the on-shell manifestations of the Adler zeros [2] predicted by PCAC at the unphysical point $s = t = u = m_\pi^2$. Such predictions are modified by unitarity corrections, which if the $S$-wave scattering lengths are small should be relatively unimportant. It is because $\pi\pi$ amplitudes are small close to threshold that the corresponding scattering lengths are hard to extract from data and we have to resort to methods based on dispersion relations. A prime aim of these is to fix low energy parameters and to establish relations between them.

The only reliable starting point for such an approach is fixed-$t$ dispersion relations. The form of these depends on the amplitude and its asymptotics. General theorems [11] require the amplitude to be bounded by $|\, s \,|^2$ for $|\, s \,| \to \infty$ for $t \leq 4m_\pi^2$. Thus at most two subtractions are needed in writing a dispersion relation, so

$$T^{sI}(s,t) \;=\; a(t) \,+\, sb(t) \,+\, \frac{s^2}{\pi}\int_{4m_\pi^2}^{\infty} ds'\,\frac{\mathrm{Im}T^{sI}(s',t)}{s'^2(s'-s)} \,+\, \frac{s^2}{\pi}\int_{4m_\pi^2}^{\infty} du'\,\frac{\sum_{I'} C^{su}_{II'}\;\mathrm{Im}T^{uI'}(u',t)}{u'^2(u'-u)} \tag{10}$$

where $a(t) \;=\; T^{sI}(0,t)$, $b(t) \;=\; \partial T^{sI}(0,t)/\partial s$. Typically these subtraction terms are related to scattering lengths by considering these relations at $t=0$ or $4m_\pi^2$.

By the late sixties, experimental knowledge of $\pi\pi$ phase shifts from 500 MeV to 1 GeV (cf. Sect. 3) together with an understanding of Regge asymptotics was sufficient to allow amplitudes to be extended to threshold using dispersion relations. One of the first analyses was by Morgan and Shaw (MS) [12], who used forward dispersion relations, i.e. Eq. (10) at $t=0$, and their derivatives for such a procedure. Though the experimental $P$-wave amplitude was known to be controlled by the $\rho-$resonance, the $I=0$ $S$-wave was largely determined by its interference with this $P$-wave. Consequently, the $S$-wave has an UP-DOWN ambiguity to be referred to later and, depending on which solution was input, different threshold parameters resulted. Nevertheless, MS found that the ensuing $I=0$ and 2 scattering lengths were correlated lying along a band, subsequently to be called the *Morgan and Shaw universal curve.* An explanation for why $a_0^0$ and $a_0^2$ are strongly connected is provided by examining the sum rule obtained by writing an unsubtracted dispersion relation for the amplitude $T^{tI=1}(s,t=0)$ divided by $(s-u)$. This is guaranteed to converge assuming Regge asymptotics. Evaluating this at the $s-$channel threshold, one obtains the sum rule [2]

$$2a_0^0 - 5a_0^2 \;=\; \frac{m_\pi^2}{8\pi^2}\int_{4m_\pi^2}^{\infty} \frac{ds}{s(s-4m_\pi^2)}\left[\;2\mathrm{Im}\;T^{s0}(s,0) \,+\, 3\mathrm{Im}\;T^{s1}(s,0) - 5\mathrm{Im}\;T^{s2}(s,0)\;\right]\,. \tag{11}$$

With experimental inputs, this typically gives [13]

$$2a_0^0 - 5a_0^2 = \;0.66 \pm 0.05 \tag{12}$$

for $0 \leq a_0^0 \leq 0.3$ again in pion mass units. About half the numerical answer comes from the $\rho-$contribution and the other half from a combination of $S-$waves and high energy inputs — the energy region determining the $S-$wave contribution depending on the particular

[2]if the normalization looks unfamiliar, this is because we here follow chiral practitioners and make our amplitudes $32\pi$ times larger than is common in discussion of such sum rules.

solution. Eq. (12) provides the correlation between the $S-$wave scattering lengths for small values of these. For larger values the low energy contribution to the dispersive integral becomes more important and the relation ceases to be linear (see Fig. 9 later). A similar evaluation [14] of the $P-$wave scattering length yields

$$a_1^1 = 0.040 \pm 0.005 \; . \tag{13}$$

Fixed-$t$ dispersion relations naturally embody $s-u$ crossing symmetry of $\pi\pi$ amplitudes. By the clever use of the 3-channel $s-t-u$ crossing properties, Roy [15] was able to write a system of equations for partial waves. Typically, the Roy equations have the form

$$T_J^I(s) = \lambda_J^I(s) + \sum_{I'=0}^{2} \sum_{J'=0}^{\infty} \int_{4m_\pi^2}^{s_{max}} K_{JI}^{J'I'}(s,s') \, \mathrm{Im}\, T_{J'}^{I'}(s') ds' \; . \tag{14}$$

The $\lambda_J^I(s)$ combine a subtraction term enforcing given $S$-wave scattering lengths, $a_0^I$, and *driving terms* carrying contributions from high energies and higher partial waves [16]. The $K$'s are known kernels. When combined with partial wave unitarity these equations neatly encapsulate the proven S-matrix constraints. The phenomenology resulting from these requirements will be discussed later in Sect. 4.

(b) Constraints for other processes leading to $\pi\pi$ final states

We confine our remarks to the simplest case of a weak or electromagnetic (production) process leading to a specific $\pi\pi$ final state with no inelasticity; a simple example would be $\gamma\gamma \to \pi\pi$. Unitarity requires that the production amplitudes should have the same **phase** as the $\pi\pi$ final state. Analyticity demands that **rapid** phase variations translate into variations of the modulus. In particular resonance poles transmit to all coupled channels. This has clearcut consequences for how we learn about narrow resonances, requiring that alternative sources of information are essentially interchangeable. Thus, one cannot have a resonance that couples to a particular production process but not to others or to elastic scattering; this has sometimes been forgotten. The machinery for implementing the universality of final state interactions by means of the Omnès function [17] is detailed in [18], for example. This interconnection allows production information to supplement elastic data. The method extends to cases where there are several two-body final states as illustrated by analysis of the $f_0(980)$ [19].

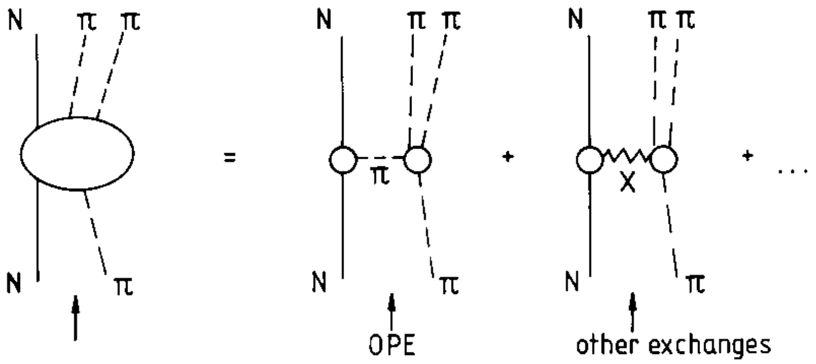


Figure 3: One-pion-exchange (OPE) and other contributions to peripheral dipion production.

What the above considerations do not deliver is any model-independent recipe for extracting slowly varying phase shifts from the modulus variation of production amplitudes. Schemes such as the isobar model that appear to provide such a linkage do not yield reliable phase shifts and hopes of extracting $\pi\pi$ phase shifts from various three body processes like $\eta \to 3\pi$ are unfounded. For processes like $\pi\pi$ (and $K\pi$) scattering, the situation is rescued by the existence of identifiable one-pion exchange signals to be discussed next. For the majority of meson-meson scattering processes like $\pi\eta$ scattering, this resource is not available.

# 3 How we know about the $\pi\pi$ interaction from experiment

Reliable information about the $\pi\pi$ interaction [7, 8, 20] comes mostly from the study of peripheral di-pion production, principally $\pi N \to \pi\pi N$ and $\pi\pi\Delta$ with emphasis on the one-pion-exchange (OPE) component of the cross-section (Fig. 3). This is inevitably accompanied by other types of exchange ($\omega, a_1, a_2, h_0$ etc, again see Fig. 3) that confuse the interpretation. Some kind of Amplitude Analysis has therefore to be performed to distinguish the OPE signal from these other effects ( which for example give quite different angular distributions for the same $J$ ). Since the beam energy has to be sufficiently high to allow a peripheral component to be identified, yet below the energies at which natural parity exchange comes to dominate over $\pi$ exchange, beam momenta in the range 7 to 50 GeV/c are preferred. Ideally, the OPE signal should be extrapolated as a function of momentum transfer, $t_{N\overline{N}}$ or $t_{N\overline{\Delta}}$, to the pion pole. Such extrapolation, advocated by Goebel and by Chew and Low [21], provides a direct measure of the $\pi\pi$ cross-section as a function of both $\pi\pi$ mass and scattering angle. However, this extrapolation is statistically very demanding and most analyses instead fit to the entire small-$t$ production cross-section assuming a simplified structure for the production amplitudes. A classic example is the method applied by Ochs and Wagner [22] to analyzing the 17 GeV/c CERN-Munich experiment on $\pi^-p \to \pi^+\pi^-n$ [23]. The method makes various factorization and coherence assumptions concerning the production amplitudes. These assumptions are partly tested via self-consistency requirements [22] and explored in experiments on polarized targets [24]. However, the main check is comparing the phases that result from applying different methods to the same data or that are derived from different processes with distinct production characteristics like $\pi N \to \pi\pi N$ and $\pi N \to \pi\pi\Delta$. As we shall see, such comparisons are mostly satisfactory. Peripheral production provides information for each $\pi\pi$ isospin and, in principle, for all partial waves with no absolute cut-off in di-meson mass. Inelastic channels can be investigated too. In practice, most information is for $M_{\pi\pi}$ below 2 GeV but above 500 MeV. There tends to be a dearth of data towards $\pi\pi$ threshold.

Other reactions provide additional data for particular sectors of the $\pi\pi$ interaction; thus, study of the reaction $e^+e^- \to \pi^+\pi^-$ helps to fix the $I = 1$ $P$-wave. A valuable source of extra information on the $I = 0$ $S$-wave phase shift, $\delta_0^0$, at low $M_{\pi\pi}$ comes from study of $K_{e4}$ decay (see [25]). This reaction has the virtue of providing model-independent information on $\delta_0^0$ close to threshold. Strictly, what is measured is the phase difference $\delta_0^0 - \delta_1^1$, but $\delta_1^1$ is taken to be known from the foregoing dispersive analysis. However, much of the hard-won information content of any $K_{e4}$ experiment goes into determining weak-interaction form-factors; the precision of the final $\delta_0^0$ determinations thus tend to be somewhat disappointing.

Other would be sources of $\pi\pi$ scattering information are either restricted in scope or highly model-dependent (at least pending substantial development of the theoretical apparatus). In recent years, central production has come to be a useful source of data about various meson systems [26], including $\pi\pi$ , and various -*onia* decays like $J/\psi \to \phi MM$ provide similar information. Such data is valuable for probing narrow resonances like $f_0(980)$ but affords essentially no constraint on slowly-varying phase shifts. Huge statistics have been accumulated in recent years on various $N\overline{N}$ annihilations leading to three meson final state like $3\pi, \pi\pi\eta, \pi\eta\eta$ and $3\eta$ [27]. Properties of the various di-meson combinations are extracted using the isobar model; methods of analysis need to be considerably refined before model-independent information can be derived. Such refinement is quite possible although laborious [28]. However, this could yield substantial benefits, for example knowledge of the low energy $\pi\eta$ phase shifts.

The same goes for the claimed extraction of $\pi\pi$ $S$-wave scattering lengths from data on $\pi N \to \pi\pi N$ near threshold [29]. In principle, $\pi N \to \pi\pi N$ near threshold is not related to low energy $\pi\pi$ scattering. However, particular models do lead to simple connections between these two processes. In this spirit, an effective Lagrangian model due to Olsson and Turner [30] has been used to extract very precise values for $a_0^0$ and $a_0^2$ from the excellent $\pi\pi N$ production data near threshold [31]. Care must be taken in interpreting these results since the extraction is model-dependent. Work is now under way to generate systematically a relation between $\pi\pi \to \pi\pi$ and $\pi N \to \pi\pi N$ at low energies based on Chiral Perturbation Theory [32]. This may provide a more dependable way of extracting $\pi\pi$ scattering lengths from these very good data.

# 4 What we know about the $\pi\pi$ interaction from experiment

We now summarize the experimental findings for $\pi\pi$ scattering below 1 GeV. For production data on di-pion final states, we principally rely on the high statistics medium energy experiments [23, 33, 34, 35, 36]. Various other experiments with lower statistics or at lower energies have also taken data [37, 38, 39, 40].. Of other $\pi^+\pi^-$ production experiments on unpolarized targets, we only mention the results of Alekseeva et al. [41]. From study of $\pi N \to 4\pi\Delta$ [42], it is concluded that the inelasticity below $K\overline{K}$ threshold is negligible.

The resulting partial wave structure is very simple in that $S$, $P$ and $D$-waves dominate below 1 GeV. The $P$ and $D$-waves are unproblematic. The $P$-wave phase shift, $\delta_1^1$, Fig. 4, is dominated by the $\rho$ resonance and the $I = 0$ $D$-wave by the tail of the $f_2(1270)$. Near

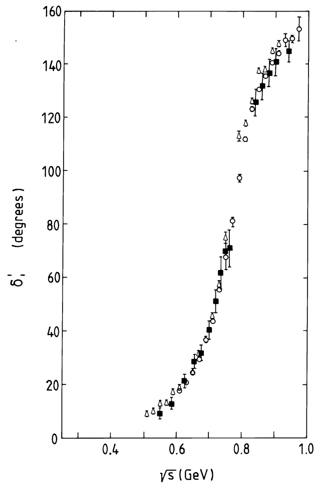


Figure 4: The $I = 1$ $P-$wave $\pi\pi$ phase shift, below 1 GeV: energy independent fits from the LBL experiment [33] (solid squares) and from separate analyses of the CERN-Munich experiment [23] by Ochs and Wagner [22] (open circles) and by Estabrooks and Martin [44] (open triangles).

threshold it is more reliable to fix both these phases by dispersion relations incorporating the above resonance dominance than to perform an energy independent phase shift analysis.

$I = 2$ phase-shifts result from studies of the production of $\pi^{\pm}\pi^{\pm}$ and $\pi^{\pm}\pi^{0}$. The charged pair experiments [35, 36, 39, 40] only allow the determination of the moduli of the phases, while $\pi^{\pm}\pi^{0}$ studies [38] show that both $\delta_0^2$ and $\delta_2^2$ are negative. Fig. 5 displays the results of the more recent high statistics experiments [35, 36], which are in mutual agreement. Certain other measurements, e.g. [40], including an earlier version of Hoogland et al.'s [43] have reported somewhat larger values. Ochs [20] points out possible defects in the way the phase shifts are extracted in some of these earlier experiments.

Information on the corresponding $I = 0$ $S$-wave phase shift, $\delta_0^0$, comes from study of both $\pi^+\pi^-$ and $\pi^0\pi^0$ production. The $\pi^+\pi^-$ experiments are mostly in very satisfactory agreement as to the general form of $\delta_0^0$ below 1 GeV. Figs. 6 and 7 compare various aspects of phase shifts derived from the high statistics CERN-Munich experiment on $\pi^-p \to \pi^+\pi^-n$ at 17 GeV/c [23] and the 7 GeV/c LBL experiment on $\pi^+p \to \pi^+\pi^-\Delta^{++}$ [33]. In addition, Fig. 6 shows results of Alekseeva et al. [41] based on a 4.5 GeV/c $\pi^-p \to \pi^+\pi^-n$ experiment ( just one of the four alternative sets of $\delta_0^0$ that they report ). Also shown are results near

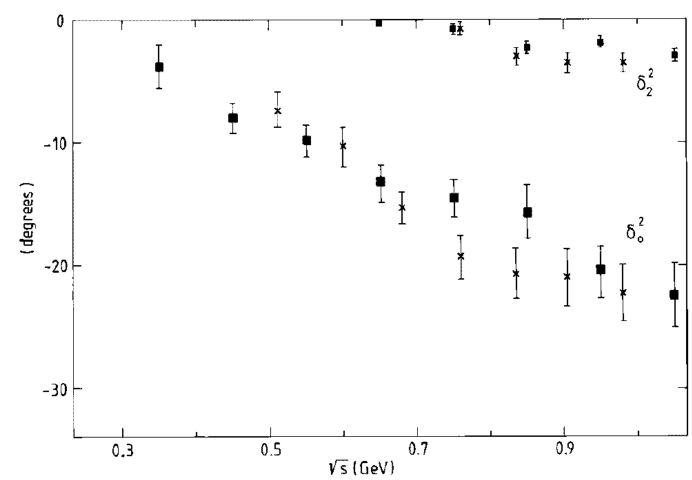


Figure 5: The $I = 2$ $S$ and $D-$wave $\pi\pi$ phase shifts, $\delta_0^2$ and $\delta_2^2$ below 1 GeV: from the CERN-Saclay [35] (crosses) and Amsterdam-CERN-Munich [36] (solid squares) experiments.

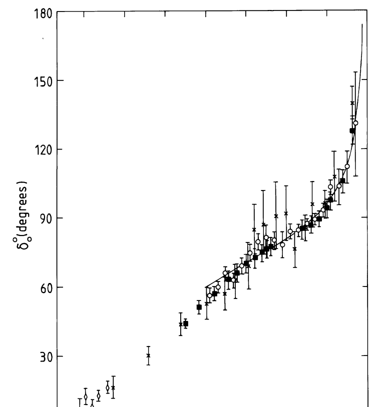


Figure 6: The $I = 0$ $S-$wave $\pi\pi$ phase shifts, $\delta_0^0$, below 1 GeV: from the LBL experiments [33] (energy dependent fit) (solid squares); from the favoured down-type solution of Alekseeva et al., [41] (crosses); from Ochs and Wagner's [22] energy independent fit (open circles) to the CERN-Munich experiment [23] — their energy dependent fit is shown as a reference curve here and in Figs. 7 and 8 labelled OW ; also from the Geneva-Saclay $K_{e4}$ decay experiment [45] (open diamonds). For more comparisons see Figs. 7 and 8.

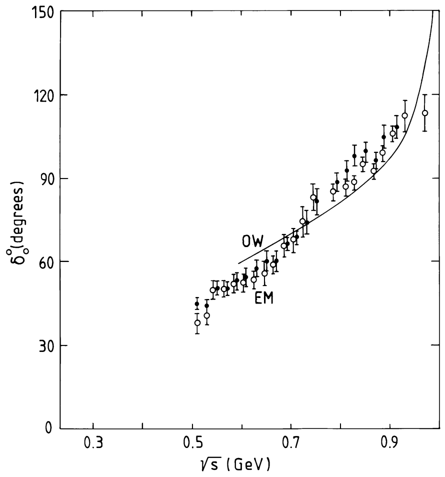


Figure 7: The $I = 0$ $S-$wave $\pi\pi$ phase shifts, $\delta_0^0$ below 1 GeV — alternative analyses of the CERN-Munich experiment [23] : Estabrooks and Martin's [44] *s-channel* (solid circles), *t-channel* (open circles) analyses EM compared to Ochs and Wagner's [22] energy dependent fit (full-line labelled OW). For other comparisons of $\delta_0^0$ data see Figs. 6 and 8.

threshold inferred from study of $K_{e4}$ decay [45] to be discussed below ( see also Fig. 11 ). The CERN-Munich experiment having the highest statistics has been analysed in several different ways. Fig. 7 compares phases from some alternative analyses. The curves in Figs. 6 and 7 show the energy dependent fit by Ochs and Wagner [22]. Fig. 7 compares this to the results of the *s-channel* and *t-channel* analyses by Estabrooks and Martin [44].

The $S$-wave in $\pi^+\pi^-$ production is principally inferred from interference with the dominant $P$-wave signal from the $\rho-$resonance. This determines $\sin(2\delta_0^0 - \delta_1^1)$ — assuming $\delta_0^2$ to be known. This quantity is invariant if $\delta_0^0(DOWN)$ is replaced by

$$\delta_0^0(UP) = \frac{\pi}{2} - \delta_0^0(DOWN) + \delta_1^1 \quad . \tag{15}$$

Prior to the high statistics production experiments [23, 33], this led to an UP-DOWN ambiguity in determinations of $\delta_0^0$ between the $\rho$ mass and 1 GeV. The UP-alternative entails a comparatively narrow $S$-wave resonance in the $\rho$ region whereas the DOWN branch yields a slowly rising $\delta_0^0$ as in Figs. 6 and 7. By common consent, the ambiguity was resolved with the DOWN alternative selected once the form of the $f_0(980)$ (alias $S^*$) was clearly delineated in $\pi^+\pi^-$ production [42, 22]. This is because the dramatic fall in the integrated cross-section and the forward-backward asymmetry near $K\overline{K}$ threshold can

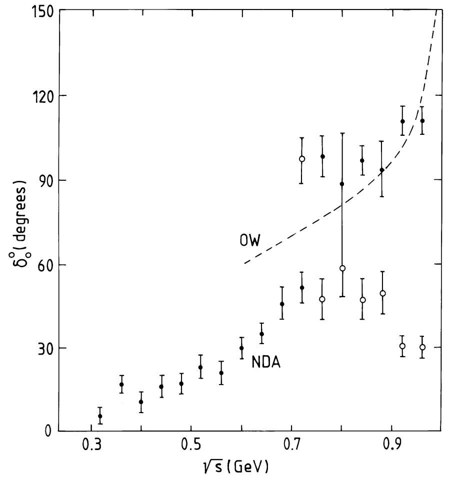


Figure 8: The $I = 0$ $S-$wave $\pi\pi$ phase shifts, $\delta_0^0$ below 1 GeV inferred from a $\pi^0\pi^0$ production experiment by the Notre Dame-Argonne group (NDA) [34], two solutions (solid circles, open circles), compared to a representative outcome from the study of $\pi^+\pi^-$ production [23] — Ochs and Wagner's energy dependent fit to the data of [22] (full line labelled OW). For other $\delta_0^0$ comparisons see Figs. 6 and 7.

only be understood if $\delta_0^0$ begins its rise through $180^o$ from $90^o$ ( see Fig. 6 ).

One might hope that study of $\pi^0\pi^0$ production would provide confirmation, but, unfortunately, the various published experiments [34, 37] disagree. In particular, the relatively high statistics experiment of the Notre Dame-Argonne group (NDA) [34] challenges the above picture and finds an UP-type form for $\delta_0^0$ below 1 GeV. The corresponding phase shifts are plotted in Fig. 8 and compared with a representative DOWN-type of solution. We do not find the NDA scenario convincing, partly from the absence of corresponding signals in central dipion production and $\gamma\gamma \to \pi\pi$, but principally because of the above argument involving the $f_0(S^*)$ signal. Data on $\pi^0\pi^0$ production through the $K\overline{K}$ threshold region with fine energy resolution would settle the issue.

Similar objections can be made to the recent claim of Svec et al. [46] to revive the UP alternative for $\delta_0^0$, on the basis of an Amplitude Analysis of their own and earlier CERN-Munich [24] $\pi^+\pi^-$ production data off polarized targets. Significantly, their analysis stops at $M_{\pi\pi} = 900$ MeV, thereby side-stepping the requirements from the form of the $f_0(S^*)$ signal. Parenthetically, we note that Pennington and Protopopescu [47] have shown that only the DOWN alternative reproduces itself through dispersion relations. Since we do not

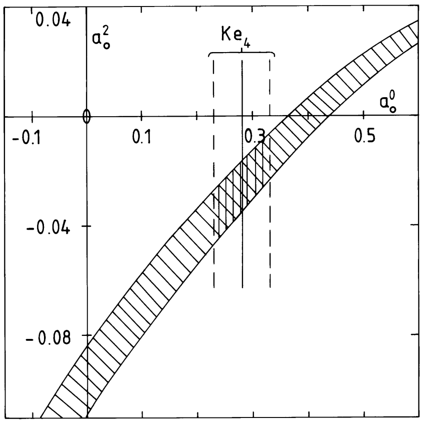


Figure 9: The Morgan and Shaw universal curve showing the correlation between the $\pi\pi$ $S-$wave scattering lengths $a_0^0$ and $a_0^2$, here obtained by fitting representative $\pi\pi$ scattering data using the Roy equations from the BFP analysis [49].

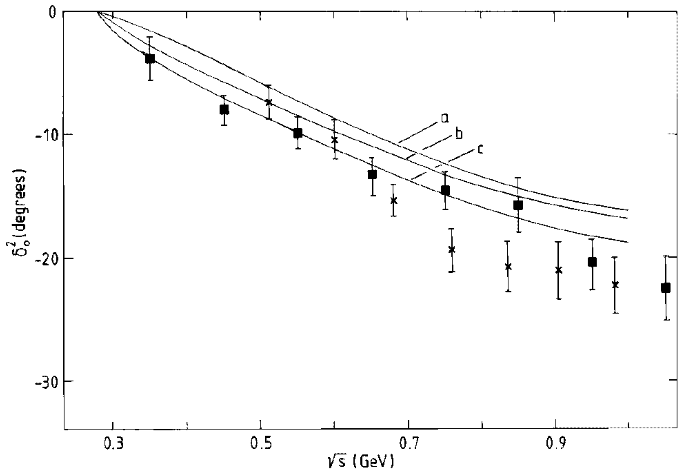


Figure 10: $I = 2$ $S-$wave $\pi\pi$ phase shifts $\delta_0^2$, below 1.1 GeV: experimental values ( legend as for Fig. 5 ) compared to BFP's fits [49] using the Roy equations (fitting $\delta_0^0$ above 500 MeV to the phases from [36]). Curves $a, b$ and $c$ correspond to alternative values for the $I = 0$ $S-$wave scattering length, $a_0^0 = 0.17$, 0.30 and 0.50.

regard either of the above claims for an UP-type as credible, we are left with the standard form shown in Figs. 6 and 7.

What these data imply about the low energy parameters beyond the earlier analysis of Morgan and Shaw [12] is provided by more sophisticated dispersive analyses using the Roy equations [15]. These are the ideal vehicle for determining the $S-$wave scattering lengths, since these are the only subtraction constants. The Roy equations require input information on all partial wave amplitudes from threshold to infinity, but being highly convergent dispersion relations they are most sensitive, when evaluated below 1 GeV, to input information below 1.2 GeV or so. At higher energies $\pi\pi$ scattering is assumed to be dominated by the well-known $f_2(1270)$ and $\rho_3(1680)$ resonances [6] with absorptive parts that average Regge exchange contributions with factorised residues. These contributions provide the so-called *driving terms* to these *partial wave* dispersion relations seen in Eq. (14). Since the integrals are twice subtracted, cf. Eq. (10), the *driving terms* are essentially quadratic in $s$ for energies below 1 GeV.

With such inputs, the Roy equations can and have been used in two ways, firstly to extend a given dataset down to threshold and secondly to map out the whole range of such extrapolations consistent with experiment. They were used in the first way by Pennington and Protopopescu [48] inputting the results of the high statistics $\pi\pi$ production experiment of the LBL group [33] with $I = 2$ information from Baton et al. [38]. When combined with partial wave unitarity, the Roy equations allow the energy dependent $S$ and $P-$wave phases of Protopopescu et al. [33] to be filled in for regions not experimentally accessed — in particular below 500 MeV. This analysis leads to values for

$$a_0^0 \,=\, 0.15 \,\pm\, 0.07 \;, \quad a_0^2 \,=\, -0.053 \,\pm\, 0.028 \tag{16}$$

in pion mass units. The errors are determined largely by the uncertainties in the $S-$wave phases. While, from such an energy dependent phase shift analysis, it is possible to assess the statistical errors, the size of the systematic uncertainties is far more difficult to judge. It is here that the yet higher statistics experiment from the CERN-Munich group [23] has been additionally useful. These data not only confirm the results of the LBL experiment, but extend our knowledge of $\pi\pi$ scattering up towards 2 GeV. It turns out that the larger event sample does not significantly decrease the errors on the $S$-wave. However, these data have been analysed in a number of different ways with differing assumptions about the

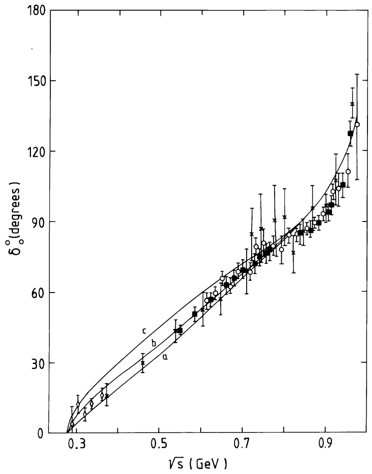


Figure 11: $I = 0$ $S-$wave $\pi\pi$ phase shifts, $\delta_0^0$, below 1 GeV: experimental values (legend as in Fig. 6) compared to BFP's fits [49] using the Roy equations, (fitting $\delta_0^0$ above 500 MeV to the phases from [44]). Curves $a, b$ and $c$ correspond to alternative values for the $I = 0$ $S-$wave scattering length $a_0^0 = 0.17, 0.30$ and $0.50$.

production mechanisms. This has allowed a better idea of the systematic uncertainties in $\delta_0^0$ as illustrated in Fig. 7.

This is the basis of the second approach to implementing the Roy equations. Basdevant, Froggatt and Petersen (BFP) [49] studied the maximum (sensible) range of $S-$wave scattering lengths allowed by a broad band of possible phase shifts. They find a correspondingly large range of scattering lengths with

$$-0.05 \; < \; a_0^0 \; < \; 0.6 \tag{17}$$

in the case of the CERN-Munich data. Their solutions map out the universal curve of MS (Fig. 9) in a systematic way. The fact that such a band correlating $a_0^0$ and $a_0^2$ exists means that there is essentially a single parameter family of extensions to threshold, which is most usefully specified by $a_0^0$.

Figs. 10 and 11 illustrate the results, respectively for $I = 2$ and 0, that BFP obtain from fitting to the Estabrooks and Martin's [44] phases above 500 MeV and for $a_0^0 = 0.17$, 0.3 and 0.5 (the corresponding curves are labelled $a, b, c$). The solutions are also compared with the representative experimental findings previously shown in Figs. 5 and 6. The $I = 2$ $S-$wave is not input in the BFP analysis, but is predicted and the comparison

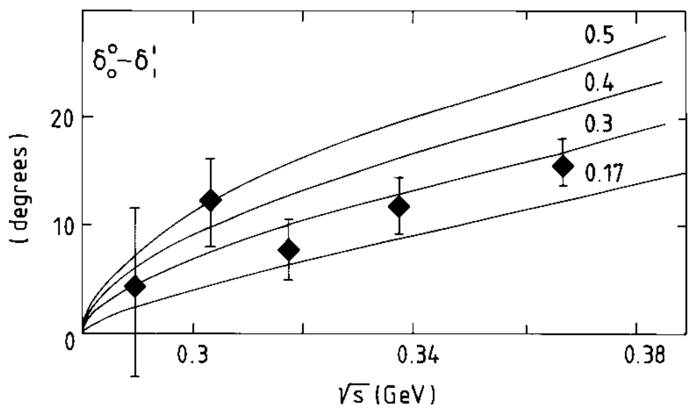


Figure 12: Results for the $\pi\pi$ phase shift difference $\delta_0^0 - \delta_1^1$ inferred from the Geneva-Saclay $K_{e4}$ experiment [45]; the curves show BFP's predictions [49], as in Figs. 10 and 11, labelled by the associated $a_0^0$ value ( 0.17, 0.30, 0.40 and 0.50 ).

with data is quite impressive (Fig. 10). However, $\delta_0^2$ does not show much sensitivity to $a_0^0$ except near threshold. As the corresponding $I = 0$ plot (Fig. 11) shows what is really needed to fix $a_0^0$ better is, as one would expect, improved $\delta_0^0$ measurements at low energies, either from further peripheral production experiments or from $K_{e4}$ decay. The best existing $K_{e4}$ data ( indicated by the diamonds in Figs. 11,12 ) are from the Geneva-Saclay experiment [45]. A free fit to these experimental phases using an effective range formula yields $a_0^0 = 0.31 \pm 0.11$ [45]. The Roy equations imply a correlation between the slope and the scattering length as illustrated by the curves in Fig. 12 for different scattering lengths from BFP [49]. Incorporating this correlation the Geneva-Saclay group quote $a_0^0 = 0.28 \pm 0.05$. This determination is shown on the $a_0^0$ $v$ $a_0^2$ plot of Fig. 9. The curves in Fig. 12 show BFP's predictions for various values of $a_0^0$.

Improved $K_{e4}$ measurements will be one way for planned DA$\Phi$NE experiments to help refine our knowledge of $a_0^0$. Prospects are discussed in [25]. Another possible route (discussed by one of us in the previous edition of this handbook [50]) would be via two-photon experiments leading to improved measurements of $\gamma\gamma \to \pi^0\pi^0$ ( and $\gamma\gamma \to \pi^+\pi^-$). DA$\Phi$NE holds out the prospect of increasing our understanding of $\pi\pi$ scattering to a significant degree.

# References


[1] For a recent review, see H. Leutwyler, contribution to the MIT Workshop on *Chiral Dynamics* (July 1994) to be published in the Proceedings, eds. A. Bernstein and B.R. Holstein.

[2] S.L. Adler, Phys. Rev. **137** (1965) B1022, **139** (1965) B1638.

[3] J. Gasser and H. Leutwyler, Nucl. Phys. **B250** (1985) 465.

[4] J. Stern, H. Sazdjian and N.H. Fuchs, Phys. Rev. **D47** (1993) 3814.

[5] For general reviews see: A. Martin, *Scattering theory: unitarity, analyticity and crossing*, Springer-Verlag, (1969).

[6] Particle Data Group, *Review of Particle Properties*, Phys. Rev. **D50** (1994) 1173.

[7] B.R. Martin, D. Morgan and G. Shaw , *Pion Pion Interactions in Particle Physics*, Academic Press, New York (1976).

[8] J.L. Petersen, *The $\pi\pi$ Interaction*, CERN 77-04 (1977).

[9] J. Gasser, Second DAΦNE Physics Handbook, eds. G. Pancheri and N. Paver (INFN, Frascati, 1995).

[10] S. Weinberg, Phys. Rev. Lett. **17** (1966) 616.

[11] A. Martin and F. Cheung, *Analyticity Properties and Bounds of the Scattering Amplitudes*, Gordon and Breach, New York (1970).

[12] D. Morgan and G. Shaw, Phys.Rev. **D2** (1970) 520 , Nucl. Phys. **B10** (1968) 261.

[13] M.M. Nagels et al., Nucl. Phys. **B147** (1979) 189.

[14] M.G. Olsson, Phys. Rev. **162** (1967) 1338.

[15] S.M. Roy, Phys. Lett **B36** (1971) 353.

[16] J.L. Basdevant, J.C. Le Guillou and H. Navelet, Nuovo Cim. **7A** (1972) 363.

[17] R. Omnès, Nuovo Cim. **8** (1958) 316.

[18] K.-L. Au, D. Morgan and M.R. Pennington, Phys. Rev. **D35** (1987) 1633.

[19] D. Morgan and M.R. Pennington, Phys. Lett. **B258** (1991) 444, Phys. Rev. **D48** (1993) 1185.

[20] W. Ochs, $\pi N$ Newsletter **3** (1991) 25 (preprint MPI-Ph/Ph 91- 35,1991).

[21] C.J. Goebel, Phys. Rev. Lett. **1** (1958) 337;
G.F. Chew and F.E. Low, Phys. Rev. **113** (1959) 1640.

[22] W. Ochs, Univ. of Munich thesis (1973);
B.Hyams et al., Nucl. Phys. **B64** (1973) 134.

[23] G. Grayer et al., Nucl. Phys. **B75** (1974) 189.

[24] H. Becker et al., Nucl. Phys. **B150** (1979) 30, **151** (1979) 46.

[25] see articles by G. Colangelo, M.Knecht and J. Stern, and by M. Ballairgeon and P.J. Franzini in Chap. 7 of the Second DA$\phi$NE Physics Handbook, eds. G. Pancheri and N. Paver (INFN, Frascati, 1995).

[26] See for example, A. Palano, Proc. IXth Int. Workshop on Photon-Photon Collisions, San Diego, 1992, eds. D.O. Caldwell and H.P. Paar (World Scientific, 1992) p.308.

[27] C. Amsler et al., Phys. Lett. **B322** (1994) 431, **B333** (1994) 277, **B342** (1995) 433;
C. Amsler, Univ. of Zurich preprint, UZH-PH-50/94, to appear in Proc. of 27th Int. Conf. on High Energy Physics, Glasgow, July 1994 and references therefrom.

[28] V.V. Anisovich, D.V. Bugg, A.V. Sarantsev and B.S. Zou, Phys.Rev. **D50** (1994) 972.

[29] H. Burkhardt and J. Lowe, Phys. Rev. Lett. **67** (1991) 2622.

[30] M.G. Olsson and L. Turner, Phys. Rev. Lett. **20** (1968) 1127; Phys. Rev. **181** (1969) 2141; Phys. Rev. **D6** (1972) 3522.

[31] M.E. Sevior et al., Phys. Rev. **D48** (1993) 3987 and references therefrom and from [29].

[32] Ulf Meissner, contribution to the MIT Workshop on *Chiral Dynamics* (July, 1994).

[33] S.D. Protopopescu et al., Phys. Rev. **D7** (1973) 1279.

[34] N.M. Cason et al., Phys. Rev. **D28** (1983) 1586.

[35] J. Losty et al., Nucl. Phys. **B69** (1974) 185.

[36] W. Hoogland et al., Nucl. Phys. **B126** (1977) 109.

[37] W.D. Apel et al., Phys. Lett. **B41** (1973) 542;
R.K. Clark et al., Phys.Rev. **D32** (1985) 1061.

[38] J.P. Baton, G.L. Laurens and J. Reignier, Phys. Lett. **B33** (1970) 528.

[39] E. Colton et al., Phys. Rev. **D3** (1971) 2028;
C.N. Kennedy et al., Nucl. Phys. **B59** (1973) 367;
N.B. Durusoy et al., Phys. Lett. **B45** (1973) 517.

[40] J.P. Prukop et al., Phys. Rev. **D10** (1974) 2055.

[41] E.A. Alekseeva et al., Zh. Eksp. Teor. Fiz. **82** (1982) 1007.

[42] M. Alston-Garnjost et al., Phys. Lett. **B36** (1971) 152.

[43] W. Hoogland et al., Nucl. Phys, **B69** (1974) 266.

[44] P. Estabrooks and A.D. Martin, Phys. Lett. **B43** (1972) 350 .

[45] L. Rosselet et al., Phys. Rev. **D15** (1977) 574.

[46] M. Svec, A. Lesquen and L. van Rossum, Phys.Rev. **D46** (1992) 949.

[47] M.R. Pennington and S.D. Protopopescu, Phys. Rev. **D7** (1973) 2591.

[48] M.R. Pennington and S.D. Protopopescu, Phys. Rev. **D7** (1973) 1429.

[49] J.L. Basdevant, C.D. Froggatt and J.L. Petersen, Nucl. Phys. **B72** (1974) 413.

[50] M.R. Pennington, DAΦNE Physics Handbook, ed. L. Maiani, G. Pancheri and N. Paver (INFN, Frascati, 1992) pp. 381-418.